

# Solitonic vortices and the fundamental modes of the “snake instability”: Possibility of observation in the gaseous Bose-Einstein condensate

Joachim Brand and William P. Reinhardt

*Department of Chemistry, University of Washington, Seattle, Washington 98195-1700*

(Received 29 May 2001; published 1 April 2002)

The connection between quantized vortices and dark solitons in a waveguidelike trap geometry is explored in the framework of the nonlinear Schrödinger equation. Variation of the transverse confinement leads from the quasi-one-dimensional (1D) regime, where solitons are stable, to 2D (or 3D) confinement, where soliton stripes are subject to a transverse modulational instability known as the “snake instability.” We present numerical evidence of a regime of intermediate confinement where solitons decay into single, deformed vortices with solitonic properties rather than vortex pairs as associated with the “snake” metaphor. Further relaxing the transverse confinement leads to the production of two and then three vortices, which correlates perfectly with a Bogoliubov stability analysis. The decay of a stationary dark soliton (or, planar node) into a single solitonic vortex is predicted to be experimentally observable in a 3D harmonically confined dilute-gas Bose-Einstein condensate.

DOI: 10.1103/PhysRevA.65.043612

PACS number(s): 03.75.-b, 05.45.Yv, 42.65.Tg

Solitons and quantized vortices are fundamental excitations of nonlinear media. Quantized vortices, often regarded as an indicator for superfluidity, are topological defects in (2+1)- or (3+1)-dimensional fluids. Dark solitons in their purest form are solitary, nondispersive density-notch solutions to (1+1)-dimensional, nonlinear wave equations with extraordinary stability properties. It has been known, however, for many years that solitonic wave fronts (also called band solitons or soliton stripes) in two- or three-dimensional media are unstable [1–5]. The metaphor of a “snake” instability (SI) has been introduced in this context by Zakharov and Rubenchik [1] in order to refer to the antisymmetric modulation (bending) of the solitonic wave front caused by long-wavelength perturbations [3]. Later it has been predicted by numerical studies of time evolution that the SI eventually leads to the formation of arrays of vortices with alternating charge [2,4]. The first experimental evidence of the SI and subsequent formation of vortices was observed in nonlinear optics [6,7].

More recently, dark solitons have been observed in trapped dilute-gas Bose-Einstein condensates (BECs) [8], and the decay of a stationary soliton into closed loops of vortex filaments, much resembling smoke rings, has been observed in a spherical harmonic trap [9]. Stationary dark solitons, like the example shown in Fig. 1(a), are nodes (nodal lines or planes in 2D or 3D, respectively) in the wave function as opposed to traveling solitons, which are also referred to as gray solitons. Theoretically, the stability of stationary solitons in harmonically trapped BECs had been investigated before by Muryshev *et al.* [10] and Feder *et al.* [11], based on a linear stability analysis using the Bogoliubov equations. While both papers identify a regime of stability for stationary solitons in elongated traps at low density as expected from earlier work [3], it was conjectured in Ref. [10] that the mechanism of instability at increasing density was vortex pair production in analogy to the SI. Feder *et al.* [11] refined and partially corrected the results of Ref. [10] and predicted the later experimentally observed vortex ring

formation [9]. The mechanism of decay at the onset of instability, however, has not been fully revealed so far.

In this paper we study the modes of instability of a stationary soliton as a function of the transverse confinement  $L_{\perp}$ , measured in terms of the condensate healing length  $\xi$  [12,13]. The onset of instability at  $L_{\perp} \approx 6\xi$  is initiated by the emergence of a nontrivial stationary state [see Fig. 1(b)] of lower energy than the corresponding stationary soliton. We call this state a solitonic vortex (SV). A solitonic vortex is a single confined and deformed vortex with solitonic proper-

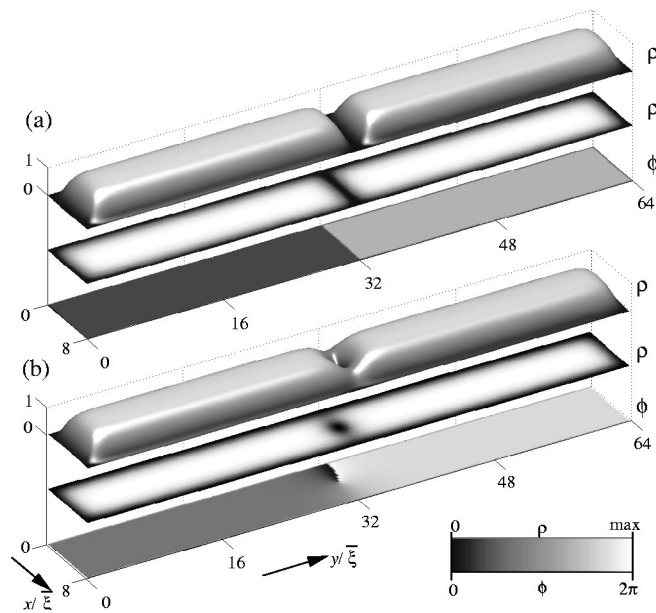


FIG. 1. Two stationary “one-defect” excited states in a 2D rectangular box trap with hard-wall boundary conditions generated by imaginary-time propagation of the nonlinear Schrödinger equation: (a) stationary soliton (line node) and (b) stationary solitonic-vortex state. The complex wave function  $\psi$  is represented by the density  $\rho = |\psi|^2$  and the phase  $\phi = \arg(\psi)$ . Each subplot shows a surface plot and gray-scale coded plots of the density and the phase modulo  $2\pi$ .

ties [13]. For transverse confinements of  $6\bar{\xi} \lesssim L_t \lesssim 10\bar{\xi}$  the strong coupling of the stationary soliton to the more stable single SV is the only decay mechanism available, in contrast to what has been seen and expected in earlier work [3,9–11]. The SV therefore, presents the smallest possible unit of decay, which persists in geometries where the transverse confinement is too tight for vortex-ring (in 2D, vortex pair) formation. Under less restrictive confinement, two and then three vortex channels open (for  $L_t \gtrsim 10\bar{\xi}$  and  $L_t \gtrsim 13\bar{\xi}$ , respectively). The one, two, and three vortex instabilities will be seen to correlate perfectly with a Bogoliubov stability analysis.

The essential physics involved reveals itself from the studies of the time-dependent Gross-Pitaevskii or nonlinear Schrödinger equation (NLSE), which presents the relevant mean-field theory for a zero-temperature BEC [14] and also applies to nonlinear wave propagation in optics [15],

$$i\partial_t\psi = [-\nabla^2 + V + gv_B|\psi|^2]\psi. \quad (1)$$

In the dimensionless Eq. (1), the condensate wave function  $\psi(\mathbf{r}, t)$  satisfies the following normalization condition:  $\int_{v_B} |\psi|^2 d\mathbf{r} = 1$ , where  $v_B$  is the volume of a box containing the trapped condensate. The external trapping potential is given by  $V$  and  $g$  is the nonlinear coupling constant. We restrict ourselves to a repulsive nonlinearity (or defocusing NLSE)  $g > 0$ . The relevant size scale for nonlinear structures like solitons [15] and vortices [16] is the condensate healing length  $\xi = 1/\sqrt{gv_B}|\psi|^2\bar{\xi}$ , where  $\bar{\xi} = 8\pi aN/(gv_B)$  is the unit of length used in Eq. (1) for a BEC with  $N$  particles and an  $s$ -wave scattering length  $a$ . Note that for fairly uniformly distributed condensates, the healing length is given by  $\bar{\xi} = 1/\sqrt{g}\xi$ . The application of NLSE solutions of the type shown in Fig. 1 has been fully confirmed empirically by the experiments of Refs. [8,9]. In tightly confined BECs, the current mean-field theory is justified as long as the transverse dimensions are greater than  $\xi$  and  $\bar{\xi} \gg a$  is satisfied (see [17]).

We initially consider a 2D rectangular geometry where the trapping potential  $V$  is represented by box boundary conditions. The chosen aspect ratio, length/width, of 8 simulates a transversely confined, waveguidelike geometry. The stationary vortexlike state with a node and phase singularity at the trap center was found by imaginary-time propagation and confirmed by real-time propagation of the NLSE [13]. In addition to seeding this relaxation procedure with a suitable phase profile, we also restricted the symmetry of the density  $|\psi|^2$  to be even in both spacial directions. A second stationary state (a dark band soliton) was also generated by imaginary-time propagation with the constraint of odd symmetry in the longitudinal direction of the trap. Figure 1 shows the resulting wave functions. The vortexlike wave function of Fig. 1(b) is clearly distorted and affected by the tight transverse confinement of  $8\bar{\xi}$ . We have argued in Ref. [13] that such a tightly confined vortex acquires solitonic properties and, therefore, should be called a solitonic vortex, further discussed in [18].

Figure 2(a) shows the excitation energy of the stationary SV and soliton state with respect to the ground state as a

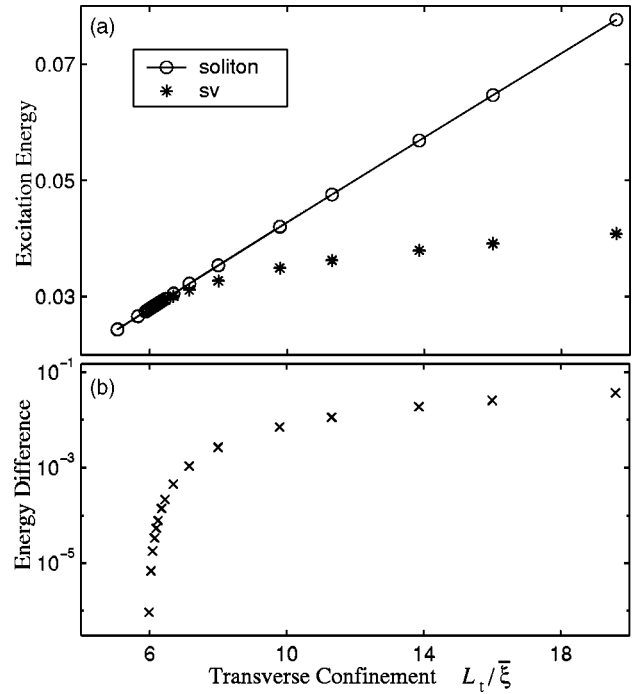


FIG. 2. SV and soliton properties as a function of the transverse confinement  $L_t$ . Part (a) shows the excitation energies of the stationary soliton and SV state. The energy difference is shown on a logarithmic scale in part (b). The simulations were done in a rectangular box of size  $8\bar{\xi} \times 64\bar{\xi}$  for different values of the nonlinear coupling constant  $g$ , which changes the effective transverse confinement  $L_t/\bar{\xi} = 8\sqrt{g}$ .

function of the transverse confinement  $L_t$  in terms of  $\bar{\xi}$ . For a given wave function  $\psi$ , the energy is given by the formula  $E = \int_{v_B} (-\psi^* \nabla^2 \psi + gv_B/2 |\psi|^4 + V |\psi|^2) d\mathbf{r}$ . The soliton-excitation energy exhibits a linear dependence on the variation of the length scale reflecting the localization of the excitation in one and extension in the other spacial dimension. The SV energy is always lower than the soliton energy and grows more slowly with the box size, reflecting the expected logarithmic behavior for large boxes [16]. Below a critical confinement corresponding to a box width of  $\approx 6\bar{\xi}$  we do not find any stationary SV solutions but instead the imaginary-time propagation converges to the soliton solution. The logarithmic plot of the energy difference between the soliton and the SV energies shown in Fig. 2(b) very much indicates a nonanalytic curve joining or curve crossing. Following the SV solution from wide confinement to the critical point, the vortex wave function shows an increasingly deformed density and squeezed phase signature (see Fig. 1) and eventually coincides with the soliton wave function at the critical confinement.

The band solitons and SV states from Fig. 2(a) are stationary states. In wide enough confinement, however, band solitons may exhibit the SI mentioned earlier: Tiny imperfections of stationary band solitons may lead to a transverse modulation and grow during real-time propagation at an initially exponential rate. The stability of the stationary solutions of the NLSE can be tested in a linear stability analysis

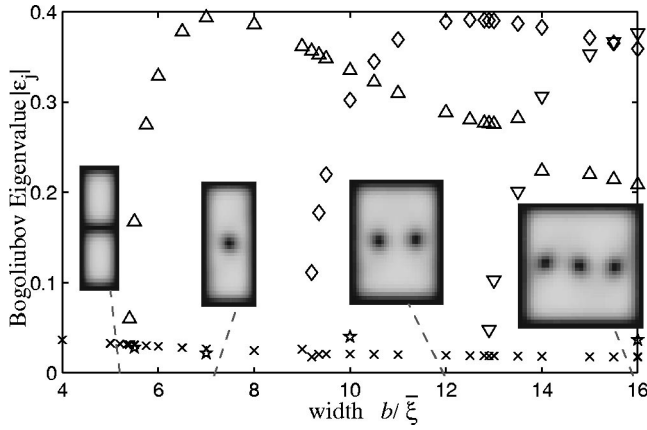


FIG. 3. Bogoliubov spectrum of the stationary soliton in a 2D box as a function of the box width at constant average density. The insets relating to box widths of  $b = 7\bar{\xi}$ ,  $12\bar{\xi}$ , and  $16\bar{\xi}$  show density plots of transient patterns in the decay of the perturbed soliton state (see text) after real-time propagation for  $t = 26, 31$ , and  $26$  in the units of Eq. (1), respectively. The perturbed soliton at  $b = 5\bar{\xi}$ , on the contrary, shows no appreciable decay after 100 time units. The imaginary modes are marked according to the nature of the eigenvector  $u$  leading to single-vortex ( $\Delta$ ), double-vortex ( $\diamond$ ), or triple-vortex ( $\nabla$ ) decay. The anomalous modes of the nodal-plane state ( $\times$ ) and stationary single-svortex state ( $\star$ ) are also indicated.

employing the famous Bogoliubov equations [19], which can be derived from a linear-response expansion of the time-dependent NLSE [20]. In the units of Eq. (1) these equations read

$$\mathcal{L}u_j(\mathbf{r}) - gv_B[\psi(\mathbf{r})]^2v_j(\mathbf{r}) = \epsilon_j u_j(\mathbf{r}), \quad (2)$$

$$\mathcal{L}v_j(\mathbf{r}) - gv_B[\psi^*(\mathbf{r})]^2u_j(\mathbf{r}) = -\epsilon_j v_j(\mathbf{r}), \quad (3)$$

with  $\mathcal{L} = -\nabla^2 + V(\mathbf{r}) + 2gv_B|\psi(\mathbf{r})|^2 - \mu$ , and  $\mu$  is the chemical potential of the stationary wave function  $\psi(\mathbf{r}, t) = \exp(-i\mu t)\psi(\mathbf{r})$ . The solutions of the Bogoliubov equation with eigenvalues  $\epsilon_j$  and eigenvectors  $(u_j, v_j)$  have the following interpretation in terms of small-amplitude motion around a stationary solution of the NLSE [16]: Small positive  $\epsilon_j$  at positive “norm”  $\eta_j = \int (|u_j|^2 - |v_j|^2) d\mathbf{r}$  describe small oscillations around the stationary state with increasing energy. Solutions with negative eigenvalues  $\epsilon_j$  and positive  $\eta_j$  are called anomalous modes. They indicate a continuous transformation of the stationary state to a state of lower energy. Anomalous modes exist for the trapped vortex as well as for dark solitons in 1D and merely express the thermodynamic instability of these excitations. Complex or purely imaginary eigenvalues  $\epsilon_j$ , however, indicate a dynamical instability. They further imply  $\eta_j = 0$  [16,21].

Figure 3 shows the purely imaginary and anomalous eigenvalues of the Bogoliubov equation for a stationary band soliton in a rectangular box of dimension  $b \times 16\bar{\xi}$  as a function of the box width  $b \approx L_t$  at constant density. For narrow traps with  $b \lesssim 5.5\bar{\xi}$ , we find one anomalous but no complex eigenvalues, like for 1D solitons. Additionally, the soliton wave function shows no appreciable decay in real-time

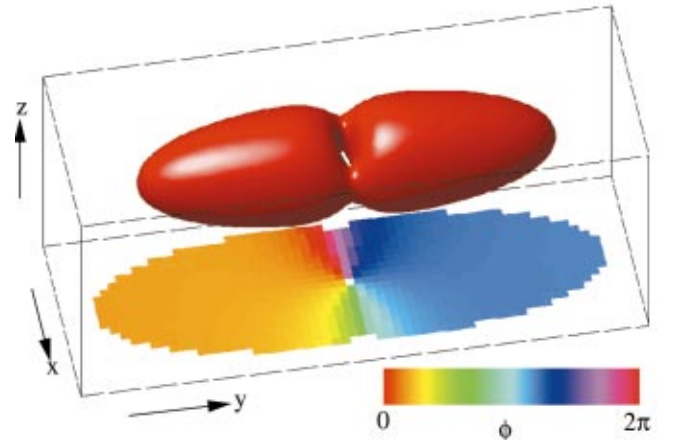


FIG. 4. (Color) SV in a 3D elongated harmonic trap generated by decay of a perturbed stationary soliton state. Shown is the surface of constant density (at 0.16 of the maximum density) and a color-coded plot of the phase in the horizontal plane intersecting the trap center. The transverse confinement  $L_t/\bar{\xi} \approx 7.7$  was computed by the maximum value of the line integral  $\int_C \xi(\mathbf{r})^{-1} ds$  taken along the transverse dimension, which is more appropriate for measuring the transverse confinement of inhomogeneous condensates than the box width [13]. For details of the simulation see text.

propagation seeded with noise (see insets). Also collisions of noisy gray solitons show the robust, particlelike behavior expected from 1D soliton theory [18]. For trap widths  $5.5\bar{\xi} \lesssim b \lesssim 9.5\bar{\xi}$ , one purely imaginary eigenvalue exists in the Bogoliubov spectrum. According to the numerical results, the emergence of this imaginary eigenvalue coincides with the emergence of the SV as a symmetry-breaking stationary state of lower energy than the corresponding band soliton. Increasing the box width, a second and eventually a third imaginary eigenvalue appears. The stability of the stationary soliton was probed using real-time propagation seeded with 0.01% white noise [22]. While there is no appreciable decay in tight confinement, we clearly find that the soliton instability is associated with the formation of one, two, and three vortices in the regimes where one, two, and three imaginary eigenvalues are present as shown in the insets of Fig. 3. The eigenvectors  $u_j$ , localized within about one healing length from the nodal line of the soliton, also support this result [18]. The patterns shown in Fig. 3 are by no means stationary but rather form transient states followed by incomplete recurrences of the nodal line and eventual further decay where vortices move to the edge of the trap and vorticity is destroyed. The complicated dynamical patterns showing a mixture of decay and strong mode coupling are certainly due to energy conservation in the NLSE and to the small scale of the trap used in the simulation where radiated phonons linger. We expect further stabilization of the vortex patterns in longer traps where energy released in the decay process can distribute itself over a larger area. The observed decay patterns vary depending on the exact form of the initial perturbation by noise. In contrast to the soliton, the stationary SV shows an entirely real Bogoliubov spectrum with one anomalous mode also shown in Fig. 3. Further, real-time propagation of perturbed SVs shows no appreciable de-

cay. In this sense, the SV is the more stable object than the stationary soliton.

Finally, we would like to comment on the 3D harmonic-trap geometry studied earlier in the experiment by Anderson *et al.* [9] and in theoretical work by Muryshev *et al.* [10] and Feder *et al.* [11]. Both experiment [9] and theory [11] report vortex-ring formation during the decay of a stationary soliton (nodal-plane state) in spherical [9,11] and elongated [11] geometries at fairly high densities, which is indicated by the nature of complex modes in the Bogoliubov spectrum of the stationary soliton [11]. It has also been pointed out that the Bogoliubov spectrum becomes entirely real at sufficiently low particle number or high aspect ratio in elongated traps. However, the decay mechanism in the presence of a single imaginary mode (as shown in Fig. 4 of Ref. [11]) of a stationary soliton in an elongated trap has not been revealed so far. Imaginary- and real-time propagation clearly show that a stationary SV solution exists in this regime and that it has lower energy than the stationary soliton. The density and phase profile of the stationary SV state are very similar to the dynamically generated pattern shown in Fig. 4. This figure shows the transient decay product of a perturbed stationary black soliton after real-time propagation for 100 ms, seeded initially with 0.01% white noise. The parameters and potential  $V$  of this 3D harmonic trap ( $N=10^4$  atoms of Na) corre-

spond to Fig. 4 of Ref. [11] at an aspect ratio of  $\omega_\rho/\omega_x=4$  with  $\omega_x=2\pi\times 50$  rad/s. The corresponding imaginary Bogoliubov mode  $u_j$  has an azimuthal coordinate dependence of  $\exp(i\phi)$ , where  $\phi$  is the azimuthal angle, and much resembles the first imaginary mode in the 2D box discussed above. The predicted decay of the band soliton into a single SV has not been seen, or predicted, before and should be easily observable with current experimental techniques.

Concluding, we have identified the fundamental modes of the SI for transversely confined geometries: Production of one, two, and three vortices correlates with imaginary modes in the Bogoliubov eigenvalue spectrum. Departure from the quasi-1D regime of stability of solitons is indicated not only by a linear stability analysis but also by the emergence of a solitonic vortex as a stationary state of lower energy than the corresponding dark soliton. We demonstrated that the decay of a soliton into a single svortex is a fundamental mode of instability in 2D box geometry and 3D elongated harmonic traps.

We would like to thank Yuri Kivshar for a discussion and David Feder for helpful comments and access to unpublished results. Support from the National Science Foundation and the Alexander von Humboldt Foundation (J.B.) is gratefully acknowledged.

- 
- [1] V. E. Zakharov and A. M. Rubenchik, Zh. Éksp. Teor. Fiz. **65**, 997 (1973) [Sov. Phys. JETP **38**, 494 (1974)].
- [2] C. A. Jones, S. J. Putterman, and P. H. Roberts, J. Phys. A **19**, 2991 (1986).
- [3] E. A. Kuznetsov and S. K. Turitsyn, Zh. Éksp. Teor. Fiz. **94**, 119 (1988) [Sov. Phys. JETP **67**, 1583 (1988)].
- [4] C. T. Law and G. A. Swartzlander, Jr., Opt. Lett. **18**, 586 (1993).
- [5] Y. S. Kivshar and D. E. Pelinovsky, Phys. Rep. **331**, 117 (2000).
- [6] A. V. Mamaev, M. Saffman, and A. A. Zozulya, Phys. Rev. Lett. **76**, 2262 (1996); A. V. Mamaev *et al.*, Phys. Rev. A **54**, 870 (1996).
- [7] V. Tikhonenko, J. Christou, B. Luther-Davies, and Y. S. Kivshar, Opt. Lett. **21**, 1129 (1996).
- [8] J. Denschlag *et al.*, Science **287**, 97 (2000); S. Burger *et al.*, Phys. Rev. Lett. **83**, 5198 (1999).
- [9] B. Anderson *et al.*, Phys. Rev. Lett. **86**, 2926 (2001).
- [10] A. E. Muryshev, H. B. van Linden van den Heuvell, and G. V. Shlyapnikov, Phys. Rev. A **60**, R2665 (1999).
- [11] D. Feder *et al.*, Phys. Rev. A **62**, 053606 (2000).
- [12] W. P. Reinhardt and C. W. Clark, J. Phys. B **30**, L785 (1997).
- [13] J. Brand and W. P. Reinhardt, J. Phys. B **34**, L113 (2001).
- [14] F. Dalfovo, S. Giorgini, L. P. Pitaevskii, and S. Stringari, Rev. Mod. Phys. **71**, 463 (1999).
- [15] Y. S. Kivshar and B. Luther-Davies, Phys. Rep. **298**, 81 (1998).
- [16] A. L. Fetter and A. A. Svidzinsky, J. Phys.: Condens. Matter **13**, R135 (2001).
- [17] D. S. Petrov, G. V. Shlyapnikov, and J. T. M. Walraven, Phys. Rev. Lett. **85**, 3745 (2000).
- [18] J. Brand and W. P. Reinhardt (unpublished).
- [19] N. Bogolubov, J. Phys. (Moscow) **11**, 23 (1947).
- [20] M. Edwards *et al.*, Phys. Rev. Lett. **77**, 1671 (1996).
- [21] D. V. Skryabin, Phys. Rev. A **63**, 013602 (2001).
- [22] L. D. Carr, J. N. Kutz, and W. P. Reinhardt, Phys. Rev. E **63**, 066604 (2001).